Developmental Cell, Vol. 3, 697–710, November, 2002, Copyright ©2002 by Cell Press

GLD-3, a Bicaudal-C Homolog that Inhibits FBF to Control Germline Sex Determination in *C. elegans*

Christian R. Eckmann,[1,2] Brian Kraemer,[2] Marvin Wickens,[2] and Judith Kimble[1,2,3]
[1]Howard Hughes Medical Institute
[2]Department of Biochemistry
433 Babcock Drive
University of Wisconsin-Madison
Madison, Wisconsin 53706

Summary

The FBF RNA binding proteins control multiple aspects of *C. elegans* germline development, including sex determination. FBF promotes the oocyte fate at the expense of spermatogenesis by binding a regulatory element in the *fem-3* 3′UTR and repressing this sex-determining gene. Here we report the discovery of GLD-3, a Bicaudal-C homolog and cytoplasmic protein that physically interacts with FBF. Using RNAi and a *gld-3* deletion mutant, we show that GLD-3 promotes the sperm fate, a sex determination effect opposite to that of FBF. By epistasis analysis, GLD-3 acts upstream of FBF, and, in a yeast three-hybrid assay, GLD-3 interferes specifically with FBF binding to the *fem-3* 3′UTR. We propose that GLD-3 binds FBF and thereby inhibits its repression of target mRNAs.

Introduction

Mature mRNAs are extensively regulated during animal development. One type of control involves modification of the basal protein synthetic machinery; for example, phosphorylation of translation initiation factors can regulate both cell growth and specific mRNAs (Dever, 2002). A second mode of control relies on RNA binding proteins that bind specific mRNAs, often through elements in their 3′UTRs, and regulate their translation, stability, or localization (Wickens et al., 2000). This second mechanism is particularly conspicuous in the germline and early embryo. Lesions in the RNA binding protein or its RNA binding site can cause severe developmental defects, including sterility, morphological abnormalities, and lethality. In this paper, we begin to address how specific RNA binding proteins are controlled to regulate mRNAs at the correct time and place of development.

In *C. elegans*, mRNA regulation plays a major role in the decision between spermatogenesis and oogenesis (Puoti et al., 1997). The specification of a germ cell as sperm or oocyte relies on essentially the same sex determination pathway that governs male or female development in somatic tissues (Meyer, 1997). In the germline, however, that somatic pathway is modified by germline-specific regulators that control mRNA activities (Puoti et al., 1997). Normally, XX animals are hermaphrodite, making sperm first and then oocytes, and XO males make sperm continuously. In both hermaphrodites and males, the *fog-1* gene is required for specification of the sperm fate (Barton and Kimble, 1990); intriguingly, *fog-1* encodes an RNA binding protein in the CPEB family (Jin et al., 2001; Luitjens et al., 2000). Furthermore, in hermaphrodites, the transient generation of sperm is regulated by a cascade of 3′UTR controls. Thus, the female-promoting *tra-2* mRNA is repressed via a 3′UTR element to initiate hermaphrodite spermatogenesis (Goodwin et al., 1993), and the male-promoting *fem-3* mRNA is repressed via a distinct 3′UTR element to achieve the hermaphrodite switch from spermatogenesis to oogenesis (Ahringer and Kimble, 1991).

Regulation of the hermaphrodite sperm/oocyte switch has served as a paradigm for analyzing the function of the broadly conserved PUF (Pumilio and FBF) family of RNA binding proteins (Wickens et al., 2002). FBF (*fem-3* binding factor) binds the PME regulatory element in the *fem-3* 3′UTR, the *fem-3* male-promoting activity is repressed, and the germline switches from spermatogenesis to oogenesis (Zhang et al., 1997). Other PUF proteins are also 3′UTR regulators. Thus, *Drosophila* Pumilio binds the NRE regulatory elements in the *hunchback* (*hb*) 3′UTR and inhibits *hb* mRNA translation (Murata and Wharton, 1995; Wharton et al., 1998; Zamore et al., 1997). In *S. cerevisiae*, PUF-5 binds a 3′UTR regulatory element to control mating type (Tadauchi et al., 2001), a role analogous to that of FBF in *C. elegans* germline sex determination. In vertebrates, PUF functions remain unknown, but PUF proteins are present in the germline (Nakahata et al., 2001; F. Moore and R. Reijo-Pera, personal communication). Therefore, PUF proteins are broadly conserved and appear to be critical components of an ancient mechanism for mRNA regulation.

FBF is a collective term for the products of two nearly identical genes, *fbf-1* and *fbf-2*, which appear to be redundant (Zhang et al., 1997). Removal of FBF activity abolishes the hermaphrodite sperm/oocyte switch: sperm are made continuously and no oocytes are formed (Zhang et al., 1997). Therefore, FBF normally promotes oogenesis. In addition to its role in germline sex determination, FBF is also required for the process of spermatogenesis (Luitjens et al., 2000) and for maintenance of germline stem cells (Crittenden et al., 2002). Thus, FBF is critical for multiple aspects of germline development.

In this paper, we report the identification and characterization of GLD-3. The GLD-3 acronym (germline development defective) is used here because GLD-3 defects are similar, albeit not identical, to those of two previously described genes, *gld-1* and *gld-2* (Francis et al., 1995; Kadyk and Kimble, 1998; Wang et al., 2002). The GLD-3 protein was identified in a two-hybrid screen for FBF interactors; it is a KH protein, and belongs to the Bicaudal-C family of RNA binding proteins. We show that GLD-3 is a predominantly cytoplasmic protein and is required for multiple aspects of germline development, including sex determination, and for embryogenesis. Most critical for this work, GLD-3 promotes the sperm fate at the expense of oogenesis, a sex determination function opposite to that of FBF. Genetically, *fbf* is epistatic to *gld-3*, suggesting that GLD-3 is a negative

[3]Correspondence: jekimble@facstaff.wisc.edu

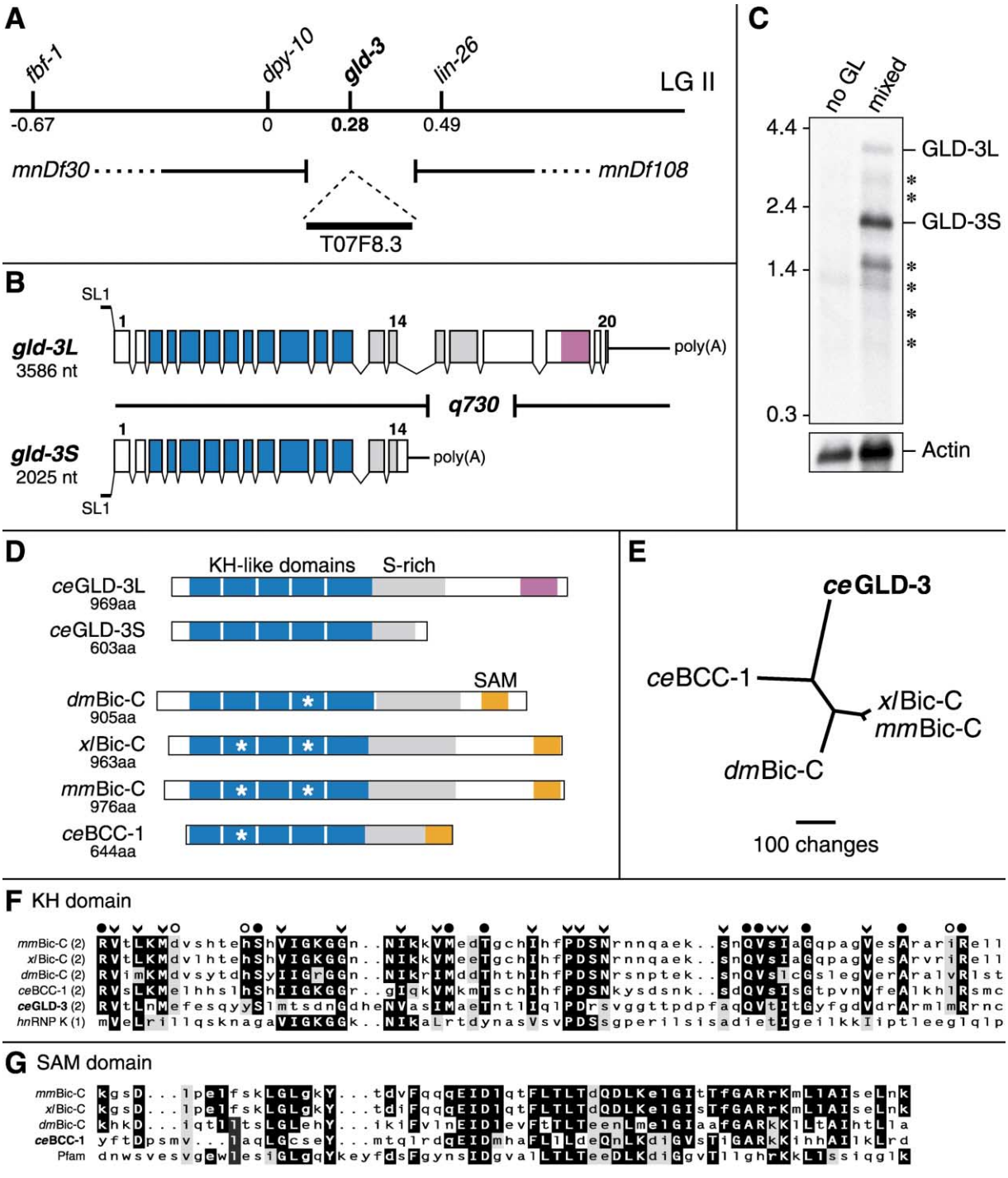

Figure 1. The *gld-3* Gene and Its Products

(A) Genetic map position. *gld-3* was defined by transcript T07F8.3, which is predicted to map genetically to position +0.28 on chromosome *II*. Neither of two deficiencies in the region, *mnDf30* (Labouesse et al., 1994) and *mnDf108* (Zalevsky et al., 1999), removes the locus.

(B) Two major *gld-3* transcripts, *gld-3L* and *gld-3S*. Boxes, exons; connecting lines, introns. Both mRNAs are SL1 *trans*-spliced to their start codons. An alternate splice site produces *gld-3S*. *gld-3L* ends in a 654 nt long 3′UTR, and *gld-3S* in a 191 nt long 3′UTR. Exons encoding GLD-3 protein motifs are color coded as in Figure 1D. Extent of the 876 bp *gld-3(q730)* deletion is indicated by a gap.

(C) Northern blot of mRNAs prepared from mixed stage wild-type hermaphrodites (mixed) or adults homozygous for *glp-1(q224)* raised at restrictive temperature, which have no germline (no GL). A cDNA probe covering exons 1–14 detects *gld-3L* and *gld-3S* as well as one major band (asterisks below GLD-3S) corresponding to a double alternatively spliced RNA that removes exons 7–13 and 16-UTR from *gld-3L*; other alternatively spliced RNAs are represented as minor bands (asterisks). Actin mRNA was used as a loading control; left, molecular weight markers (kb). Both *gld-3* transcripts are enriched in germline-containing worms. See Supplemental Data for a description of transcripts marked by asterisks.

(D) Motif organization of Bic-C proteins, drawn to scale. Blue box with white asterisk, KH-like RNA binding domain predicted by PFAM

regulator of FBF. We provide evidence that GLD-3 interferes with FBF binding to the *fem-3* PME regulatory element, and suggest that this change in the FBF/PME interaction is critical for FBF control by GLD-3.

Results

gld-3 Is a *Bicaudal-C* Homolog

To identify proteins that interact with FBF, we performed a yeast two-hybrid screen using FBF-1 as bait, analyzing 20,000,000 transformants (Kraemer et al., 1999). Among the 19 positives were two partial cDNAs corresponding to the predicted open reading frame T07F8.3; we have dubbed this gene *gld-3* (Figure 1A). The *gld-3* gene generates several mRNAs (Figures 1B and 1C), which are all *trans*-spliced to SL1. Of greatest importance here are one long mRNA, *gld-3L*, and one short mRNA, *gld-3S*; these share their first 13 exons (Figure 1B). On Northern blots, *gld-3L* and *gld-3S* were observed in poly(A)$^+$ RNAs prepared from mixed stage animals (Figure 1C, lane 2) and in staged poly(A)$^+$ RNAs throughout development (data not shown); however, they are not detected in *glp-1* mutant adults, which have essentially no germline (Figure 1C, lane 1). Therefore, *gld-3L* and *gld-3S* are likely to be expressed in the germline, an idea that is supported by analysis of GLD-3 proteins (see below). Other *gld-3*-specific bands detected on Northern blots include a variety of alternatively spliced mRNAs that have been confirmed using RT-PCR (Figure 1C, asterisks; see Supplemental Data at http://www.developmentalcell.com/cgi/content/full/3/5/697/DC1). Analysis of these other *gld-3* mRNAs is beyond the scope of this paper.

Immunoanalyses (see below) show that the *gld-3* locus encodes two major proteins, GLD-3L and GLD-3S, made from *gld-3L* and *gld-3S* mRNAs, respectively. Sequence analyses of GLD-3L and GLD-3S reveal a common region with five consecutive KH-related motifs and a serine-rich domain (Figure 1D). C-terminally, GLD-3S ends with 29 unique amino acids, while GLD-3L extends another 395 amino acids. Database searches with the GLD-3 amino acid sequences revealed weak similarity to Bicaudal-C (Bic-C) proteins (Figures 1E and 1F), and no similarity to other proteins. The standard Bic-C architecture includes five KH-related motifs followed by a serine-rich region and a SAM (sterile α motif) domain (Mahone et al., 1995; Wessely and De Robertis, 2000; Wessely et al., 2001). GLD-3 has no SAM domain, but does possess the other diagnostic motifs of the Bicaudal-C family (Figure 1D).

To determine whether the *C. elegans* genome encodes a more typical Bic-C protein, we searched Wormbase (http://www.wormbase.org) and found three predicted transcripts, M7.3, M7.4, and M7.6, which together might generate a classical Bic-C homolog. By RT-PCR, we showed that M7.3, M7.4, and M7.6 belong to the same transcript; we call this gene *bcc-1*. Comparison of the KH and SAM motif sequences revealed conservation of key amino acid residues (Figures 1F and 1G). To assess the relationships among GLD-3 and other Bic-C proteins, we examined the five KH-related motifs by exhaustive parsimony analysis (Figure 1E; see Experimental Procedures). Our results, presented as an unrooted distance tree (Figure 1E), show that both *C. elegans* Bic-C homologs are highly diverged from other Bic-C proteins. We conclude that the *C. elegans* genome possesses two Bic-C homologs: the more classical *bcc-1* and the more divergent *gld-3*. We focus here on the *gld-3* locus.

GLD-3 Is Cytoplasmic and Colocalizes with P Granules in the Early Embryo

To examine GLD-3 protein, we generated two polyclonal antibodies. One, called anti-GLD-3, was raised to the N-terminal 23 amino acids of GLD-3 and recognized both GLD-3L and GLD-3S (Figure 2A, top); the second, called anti-GLD-3L, was raised to a 368 amino acid fragment found in GLD-3L, but not GLD-3S, and recognized only GLD-3L (Figure 2A, middle). Importantly, the major proteins detected by these purified antibodies correlated in size with in vitro-translated products of cDNAs corresponding to *gld-3L* and *gld-3S* mRNAs (data not shown); therefore, the GLD-3L and GLD-3S proteins are likely to be products of the *gld-3L* and *gld-3S* mRNAs.

Wild-type adults of either sex expressed both GLD-3L and GLD-3S (Figure 2A, lanes 1 and 2). By contrast, adult *glp-1(ts)* hermaphrodites, which have virtually no germline, had no detectable GLD-3 (Figure 2A, lane 3), consistent with the idea that *gld-3* is expressed specifically in the germline. Furthermore, the deletion mutant, *gld-3(q730)*, made no detectable GLD-3 (Figure 2A, lane 4), confirming specificity of the antibodies. The *gld-3(q730)* mutant is predicted to generate an mRNA with a premature stop codon, which should be degraded by the *smg* system of nonsense-mediated decay (Pulak and Anderson, 1993). We therefore examined proteins from a *gld-3; smg-1* double mutant, but found that it too made no detectable GLD-3 (Figure 2A, lane 5). We conclude that *gld-3(q730)* is a strong loss-of-function or null mutant.

The GLD-3 subcellular distribution was investigated by immunocytochemistry. Similar results were obtained using either anti-GLD-3 (Figures 2B–2M) or anti-GLD-3L (data not shown). In most experiments, antibodies to the P granule protein PGL-1 (Kawasaki et al., 1998) were used to highlight germ cells and P granules. The data

consensus sequence PF00013; blue box without white asterisk, KH-like RNA binding domain predicted by sequence similarity; gray box, serine-rich region (S-rich); orange box, sterile α motif (SAM); violet box, minimal FBF-1 binding domain (see Figure 6).

(E) Unrooted phylogenetic tree of Bic-C family members generated by a maximum parsimony exhaustive search. Line length represents relative phylogenetic distance. Although *C. elegans* BCC-1 includes a SAM domain, which is found in most Bic-C family members but not in GLD-3, the BCC-1 amino acid sequence in the KH-like RNA binding region has diverged from other Bic-C family members almost as much as GLD-3.

(F) Alignment of amino acid sequences of second KH-like RNA binding domain of all five Bic-C family proteins; also included is the first KH domain of mammalian hnRNP K. Black boxes, identical amino acids; gray boxes, similar amino acids. Top annotations are as follows: full/empty circles are identical/similar amino acids in all five Bic-C proteins; arrowheads, identical or similar amino acids in all KH domains shown.

(G) Alignment of amino acid sequences of SAM domains compared to PFAM consensus sequence PF00536. Black boxes, identical amino acids; gray boxes, similar amino acids.

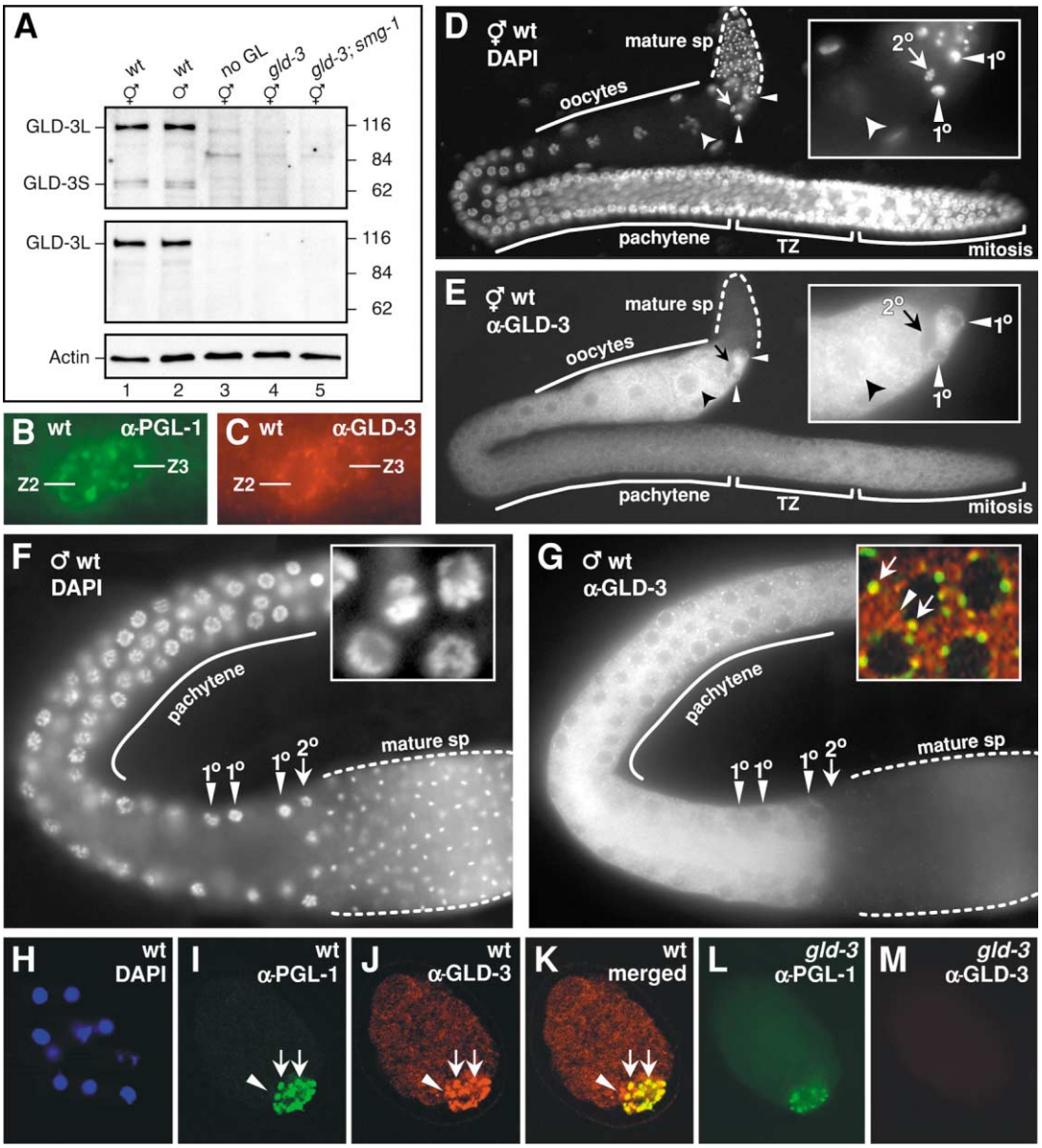

Figure 2. GLD-3 Protein during *C. elegans* Development

(A) Two GLD-3 proteins. A Western blot of proteins prepared from adult animals that were wild-type (wt) hermaphrodites (lane 1), wild-type males (lane 2), *glp-1* mutant hermaphrodites raised at restrictive temperature which lack a germline (no GL; lane 3), *gld-3(q730)* homozygous hermaphrodites (lane 4), and *gld-3(q730); smg-1* homozygous hermaphrodites (lane 5), was probed with either of two GLD-3 antibodies: anti-GLD-3 (top blot), which detects both GLD-3L and GLD-3S, or anti-GLD-3L (middle blot). Actin was used as a loading control (lower blot).

(B–M) Immunocytochemistry to determine location of GLD-3 protein. Samples shown were stained with anti-GLD-3 antibody. Similar results were obtained with anti-GLD-3L antibodies (data not shown). Epi-fluorescent images (B–H, L, and M); confocal images (I–K).

(B and C) Wild-type L1. Gonadal primordium with the two germline precursors, Z2 and Z3, stained with anti-PGL-1 (B) and anti-GLD-3 (C). For both antibodies, antigen is cytoplasmic; the nucleus is seen as a dark area in the middle of each cell.

(D–G) Extruded germlines of wild-type adult hermaphrodite (D and E) and male (F and G). DAPI (D and F); anti-GLD-3 (E and G). In both sexes, GLD-3 is predominantly cytoplasmic and present throughout the germline, except in secondary spermatocytes and mature sperm. Oocytes stain intensely with anti-GLD-3 (extent of oocytes marked by solid line; most proximal oocyte nucleus marked by small arrowhead). Primary spermatocytes also stain intensely (long arrowheads marked with 1°); secondary spermatocytes (small arrow marked with 2°) and mature sperm (extent marked by dotted line) have no detectable GLD-3. The level of GLD-3 is elevated, but not intense, in the distal germline. GLD-3 is more prominent in male pachytene than hermaphrodite pachytene germ cells, making it easier to visualize GLD-3 in granules surrounding the nuclear membrane (G). Insets in (D) and (E), 3× magnification showing GLD-3 in oocytes and primary spermatocytes. Insets in (F) and (G), 3× magnification showing early meiotic region from germlines of different males.

(F) DAPI-stained nuclei.

(G) Double stained with anti-PGL-1 (green) and anti-GLD-3 (red) antibodies. GLD-3 and PGL-1 overlap in most granules (yellow, arrow), but not all (red, *closed* arrowhead).

(H–K) Wild-type 12-cell embryo.

(L and M) Twelve-cell *gld-3(q730)* embryo from *gld-3(q730)* homozygous mother.

support three main conclusions. First, GLD-3 protein is predominantly cytoplasmic. We found GLD-3 in germline cytoplasm throughout development in both sexes (Figures 2B, 2C, 2E, and 2G, and data not shown) and in the cytoplasm of early embryos (Figures 2I–2K). Second, GLD-3 distribution is controlled spatially and temporally. In adult hermaphrodites, GLD-3 was detectable in the transition zone (TZ), where germ cells enter meiotic prophase; it was fainter in the early mitotic region and in pachytene germ cells (Figures 2D and 2E); however, as germ cells entered diakinesis, GLD-3 became abundant (Figures 2D and 2E). During spermatogenesis, GLD-3 was present in primary spermatocytes, but not in secondary spermatocytes or mature sperm (Figures 2D and 2E). A similar pattern was observed in males (Figures 2F and 2G, and data not shown). Third, GLD-3 colocalizes with P granules. P granules mark the germline throughout development, and contain proteins related to mRNA control (Seydoux and Strome, 1999). GLD-3 was found in the cytoplasm of early embryos, and colocalized with P granules from the 1-cell stage through the 64-cell stage; beyond the 100-cell stage of embryogenesis, GLD-3 was no longer detected (Figures 2H–2K, and data not shown). GLD-3 also appeared in particles that were near but not coincident with P granules (Figures 2I–2K, arrowhead). In the germline, GLD-3 was found both diffusely as well as in a more granular form (Figures 2E and 2G). The granular GLD-3 was found primarily at the cytoplasmic side of the nuclear boundary and often colocalized with PGL-1 (Figure 2G, including inset). Mutant embryos derived from *gld-3(q730)* homozygous mothers could contain apparently normal P granules that appeared to segregate normally to a single blastomere (Figure 2L); however, these *gld-3* mutant embryos had no detectable GLD-3 (Figure 2M), consistent with the idea that this mutant removes most *gld-3* activity.

gld-3 Is Required Maternally for Germline Survival and Embryogenesis

To investigate GLD-3 function, we used RNA-mediated interference (RNAi) and isolated a *gld-3* deletion mutant (*q730*; Figure 1B). Together, these two methods demonstrate that GLD-3 is required for multiple aspects of germline development and for embryogenesis. Injection of *gld-3* dsRNA into wild-type hermaphrodite germlines is predicted to reduce both maternal and zygotic *gld-3* mRNA in the progeny, which are therefore referred to as *gld-3(RNAi)* progeny. The two major *gld-3(RNAi)* defects were lethality and sterility. Lethal defects were variable, ranging from arrest at many stages of embryogenesis to arrest soon after hatching. Defects associated with sterility, on the other hand, were more uniform. The wild-type germline consists of about 1,000 "cells" organized in an elongated gonadal arm (Figures 3A and 3G). By contrast, most *gld-3(RNAi)* animals had no apparent germline (Figures 3B, 3E, and 3F). An examination of *gld-3(RNAi)* larvae showed early germline defects: germline precursor cells, Z2 and Z3, were smaller than normal in young L1s, divided more slowly than normal, and their descendants remained small and indistinct compared to their wild-type counterparts. A small cluster of faint germ cells was sometimes detected in L4 animals, but was absent in adults (data not shown). The absence of germline cells was confirmed using PGL-1 and NOS-3 antibodies (data not shown). We conclude that the *gld-3(RNAi)* germline dies in late larvae. To find whether this germline death was dependent on the canonical pathway for programmed cell death (Hengartner, 1997), we injected *gld-3* dsRNA into a *ced-3* mutant (Ellis and Horvitz, 1986). The *ced-3; gld-3(RNAi)* animals exhibited the typical *gld-3* germline survival defect (data not shown). We term this *ced-3*-independent germline death the Gls phenotype (germline survival defective). Some non-Gls *gld-3(RNAi)* hermaphrodites had stacked oocytes in a normal-sized germline (Figures 3C and 3E), a morphology typical of spermatogenesis defects. Finally, some *gld-3(RNAi)* animals had somatic defects, including a protruding vulva, multiple vulvae, or a reduction in animal size.

To distinguish between maternal and zygotic effects, we injected *gld-3* dsRNA into *rde-1* mutants, which are RNAi defective (Tabara et al., 1999). Self-progeny of genotype *rde-1; gld-3(RNAi)* were viable and fertile, indicating that *gld-3(RNAi)* relied on *rde-1* activity (Figures 3E and 3F). When the injected *rde-1* mutant hermaphrodites were crossed with wild-type males, the *rde-1/+; gld-3(RNAi)* crossprogeny possessed wild-type *rde-1*, which should render zygotic transcripts sensitive to RNAi, but leave maternal mRNAs intact. These *rde-1/+; gld-3(RNAi)* progeny were viable and generated a normal-sized germline. The simplest interpretation is that both lethality and Gls sterility, the two main defects typical of *gld-3(RNAi)* progeny, result from a loss of maternal *gld-3* function.

gld-3 Promotes Spermatogenesis

To analyze zygotic *gld-3* functions, we isolated a chromosomal deletion mutant, *gld-3(q730)*, by sib selection using a PCR-based assay (see Supplemental Procedures). This 876 nt deletion removes nearly three exons from *gld-3L* and shifts its reading frame; the deletion also removes the cleavage and polyadenylation signal from *gld-3S* (Figure 1B). All major *gld-3* mRNAs were vastly reduced in *gld-3(q730)* adults as assayed by RT-PCR (data not shown). Similarly, GLD-3 proteins were not detectable on Western blots (Figure 2A) or by immunostaining (Figure 2M). Therefore, *gld-3(q730)* is likely to be a strong loss-of-function or null mutant.

(H) DAPI.
(I and L) Anti-PGL-1.
(J and M) Anti-GLD-3.
(K) Merged image of (I) and (J) showing colocalization of GLD-3 with PGL-1 (yellow, arrows). In some granules, GLD-3 does not colocalize with PGL-1 (red, arrowhead). In *gld-3(q730)* mutant embryos that cleave, P granules are observed (L), but GLD-3 is absent (M).

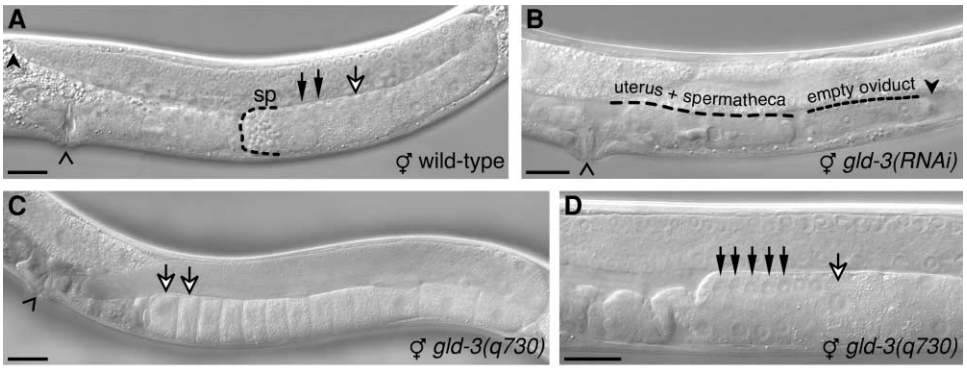

E *gld-3* germline defects in hermaphrodites

Hermaphrodite scored (20°C)	Germline defects (%) wt	Gls	Sto	other sterile	n
wild-type	100	0	0	0	>1000
gld-3(RNAi)	10	80	4	6	966
rde-1; gld-3(RNAi)	99	1	0	0	820
rde-1/+; gld-3(RNAi)	90	0	8	2	52
*gld-3(q730)**	51	0	14	35	180
gld-3(q730)	0	84	0	16	68

F *gld-3* germline defects in males

Male scored (20°C)	Germline defects (%) wt	Gls	sp + oo	other sterile	n
wild-type	100	0	0	0	>200
gld-3(RNAi)	8	68	10	14	70
rde-1/+; gld-3(RNAi)	0	0	100	0	50
gld-3(q730)	17	1	78	4	141

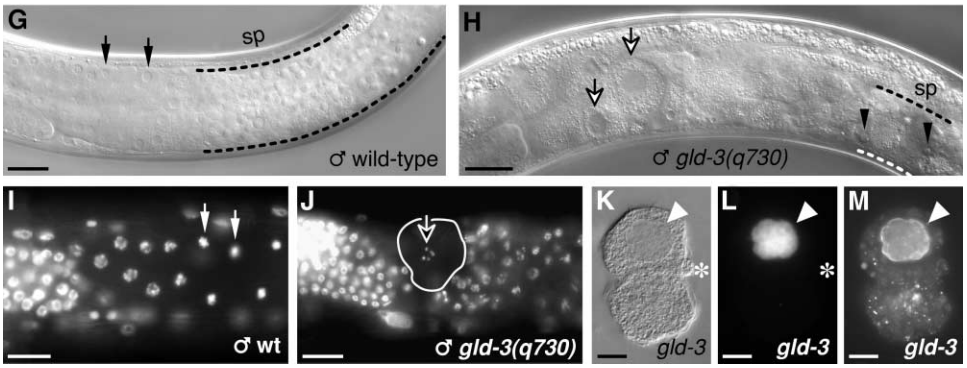

Figure 3. The *gld-3* Mutant Phenotype

(A–D and G–J) Germlines of wild-type and *gld-3*-deficient animals, visualized by Nomarski microscopy. Anterior is left; posterior is right. Closed arrows, primary spermatocytes; sp, mature sperm; open arrows, oocytes; black carat, vulva; notched arrowhead, most distal point in gonadal arm. The scale bars represent 20 μm.

(A) Wild-type adult hermaphrodite produces mature sperm and then switches into oogenesis.

(B) *gld-3(RNAi)* mutant with Gls phenotype. Most *gld-3(RNAi)* adults do not possess any germline. The somatic structures are visible and marked, but the oviduct is empty.

(C) *gld-3(q730)* mutant with Sto phenotype. Stacked oocytes indicate defective sperm, fewer sperm than normal, or no sperm.

(D) *gld-3(q730)* mutant with arrested primary spermatocytes.

(E and F) Data for defects in *gld-3*-deficient hermaphrodites (E) and males (F). *gld-3(RNAi)* progeny were scored 12–48 hr postinjection; *gld-3(q730)** hermaphrodites were homozygotes derived from a heterozygous mother; other *gld-3(q730)* animals were homozygotes derived as crossprogeny from *gld-3(q730)/+* hermaphrodites mated with *gld-3(q730)/+* males. Gls, no germline in adults; Sto, stacked oocytes; sp+oo, sperm- and oocyte-like germ cells; n, number of germline arms.

(G) Wild-type male produces sperm continuously.

(H) *gld-3(q730)* males produce oocyte-like cells (open arrows) and some sperm (dotted line and black arrowheads).

(I and J) DAPI-stained animals marked as above; the scale bars represent 20 μm.

(I) Wild-type male with nuclei in various stages of spermatogenesis.

(J) *gld-3(q730)* male. Note oocyte-like cell (circled) with chromosomal bivalents typical of oocytes (open arrow; some bivalents are out of the focal plane).

(K–M) *gld-3(q730)* embryos from *gld-3(q730)* homozygous mothers. The scale bars represent 10 μm. Nomarski (K), DAPI (L), anti-nuclear membrane antibody Mab414 (M). Most *gld-3* mutant embryos from a *gld-3* mutant mother fail in the first cell division and arrest with atypical nuclei (arrowhead). Note the unusual position of the extruded polar body, which has no DNA (asterisks in [K] and [L]). Mab414 marks nuclear membrane of one cell; the other cell has no apparent nucleus but contains Mab414-positive material dispersed throughout the cytoplasm.

We first scored *gld-3* mutant hermaphrodites for germline defects. Specifically, we examined young adults, at a time when a wild-type hermaphrodite would have switched from spermatogenesis to oogenesis. In *gld-3* mutant hermaphrodites, most spermatogenic cells were blocked as primary spermatocytes, as judged by

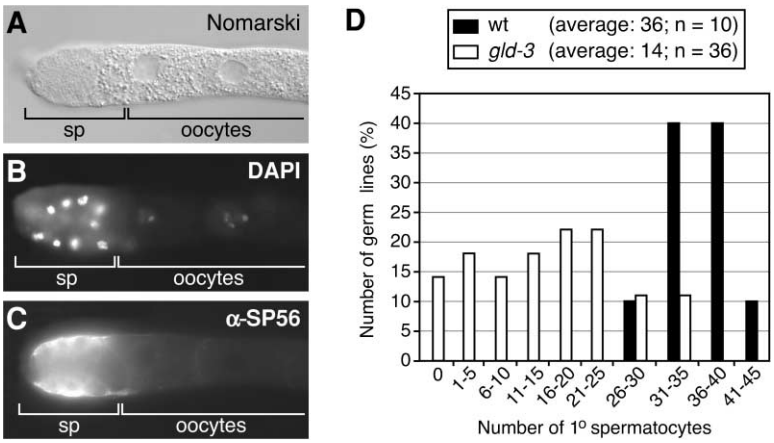

Figure 4. *gld-3* Hermaphrodites Produce Fewer Spermatocytes Than Normal

(A–C) Nomarski (A), DAPI (B), and SP56 staining (C) of a young adult *gld-3(q730)* extruded germline, focusing on its most proximal region. Germ cells committed to the spermatogenic cell fate (sp) stain positively with SP56, but are arrested as primary spermatocytes.

(D) Histogram showing number of primary spermatocytes observed in either wild-type (black bar) or *gld-3(q730)* (white bar) germlines. Wild-type hermaphrodites contained 30–41 primary spermatocytes per germline arm, whereas *gld-3(q730)* hermaphrodites produced 0–33 primary spermatocytes.

size (Figures 3D and 4A), DNA morphology (Figure 4B), and expression of the sperm-specific marker SP56 (Ward et al., 1986; Figure 4C). Arrest at the primary spermatocyte stage was not absolute, however; some secondary spermatocytes and mature sperm were seen in most animals. A similar block at the primary spermatocyte stage was also observed among *gld-3(RNAi)* hermaphrodites (data not shown). We conclude that GLD-3 promotes maturation of primary spermatocytes to mature sperm.

While scoring *gld-3* hermaphrodite germlines, we noted that the number of spermatocytes appeared to be lower than normal. To quantify this effect, we compared the number of spermatogenic cells set aside in wild-type and *gld-3* mutants (Figure 4D). In this analysis, we counted primary and secondary spermatocytes as well as mature sperm (defined by cell size, DNA morphology, and SP56 staining) in hermaphrodites with at least one but at most a few mature oocytes; we then calculated the number of primary spermatocytes represented by these various stages (Figure 4D). Whereas wild-type hermaphrodites made an average of 36 primary spermatocytes per gonadal arm ($n = 10$), *gld-3* mutants made an average of only 14 per arm ($n = 36$). Indeed, some *gld-3* gonadal arms made no spermatocytes, but instead made only oocytes. No abnormal cell death was observed in these *gld-3* mutant germlines. We interpret the decrease in the number of spermatocytes as an aberrant sperm/oocyte switch that occurred before the usual complement of spermatocytes had been set aside. An alternate interpretation might have been that the decrease in sperm number reflected a change in overall germ cell number or a delay in the onset of spermatogenesis. We have not observed any gross change in germ cell number in *gld-3* mutants, but spermatogenesis is in fact delayed by several hours. Nonetheless, in wild-type animals, allocation of normal sperm number is independent of similar delays (Kimble and White, 1981). Therefore, we conclude that GLD-3 is required during hermaphrodite development to promote the sperm fate and that this function is critical for determining the normal number of hermaphrodite sperm.

We next examined the germlines of *gld-3* homozygous males. All adult males produced some spermatogenic cells, most of which progressed from primary spermatocytes to mature sperm, although these sperm were less well defined morphologically than normal and therefore are likely to be aberrant ($n = 141$). In addition to making some sperm, most adult males produced enlarged granular cells that appeared oocyte like (Figures 3F, 3H, and 5A). This effect was also observed among *rde-1/+; gld-3(RNAi)* males (Figure 3F). Within the oocyte-like cells, chromosomal bivalents typical of oocytes were observed (Figure 3J). Similar bivalents are not seen during spermatogenesis (Figure 3I). We further assayed the oocyte-like cells using gamete-specific antibodies, and found that they stained with the oocyte-specific α-RME-2 antibody (Grant and Hirsh, 1999), but did not stain with the sperm-specific SP56 antibody (Figure 5D). Therefore, the germline is feminized in male *gld-3* mutants. We conclude that GLD-3 is required during male development for the continued production of sperm and for inhibition of oogenesis.

In addition to examining the germline of *gld-3* mutants, we also examined embryos generated by *gld-3* homozygous mothers. Some mothers produced a few fertilized embryos in addition to many unfertilized oocytes. The embryos usually arrested early, with little cleavage or nuclear division (Figures 3I–3K). When *gld-3* mothers were crossed with wild-type males, the crossprogeny either arrested during embryogenesis or grew up with no germline, the Gls phenotype. These defects mimicked the effect of *gld-3* RNAi, and confirmed their maternal nature. Therefore, GLD-3 is required maternally for early embryogenesis.

gld-3 Acts Upstream of *fbf* to Control Germline Sex Determination

To explore the regulatory relationship between FBF and GLD-3, we generated animals lacking both activities using either RNAi or deletion mutants. We focused on the epistatic relationship between these two activities in germline sex determination for several reasons. First, both FBF and GLD-3 govern germline sex determination, and they have opposite effects. Second, their sex determination defects are discrete transformations of cell fate and are easily scored. Third, effects on sex determination have been well characterized for both genes (this work; Zhang et al., 1997). These criteria are not met for other *gld-3* and *fbf* defects. One caveat to these experiments might have been that *fbf* mutants affect

A *fbf* is epistatic to *gld-3*

Animal scored	Gametes produced (%)			n
hermaphrodite	sp + oo	sp only	other sterile	
gld-3(q730)	64	0	36	188
fbf(RNAi)	0	100	0	72
fbf-1(ok91) fbf-2(q704)	0	100	0	>100
gld-3(q730); fbf(RNAi)	0	99	1	386
fbf-1(ok91) fbf-2(q704) gld-3(q730)	0	100	0	112
male	sp only	sp + oo	other sterile	
rde-1/+; gld-3(RNAi)	0	100	0	50
rde-1/+; fbf(RNAi)	99	0	1	438
rde-1/+; gld-3(RNAi); fbf(RNAi)	100	0	0	376
gld-3(q730)	17	78	5	141
fbf-1(ok91) fbf-2(q704)	100	0	0	50
fbf-1(ok91) fbf-2(q704) gld-3(q730)	99	0	1	98

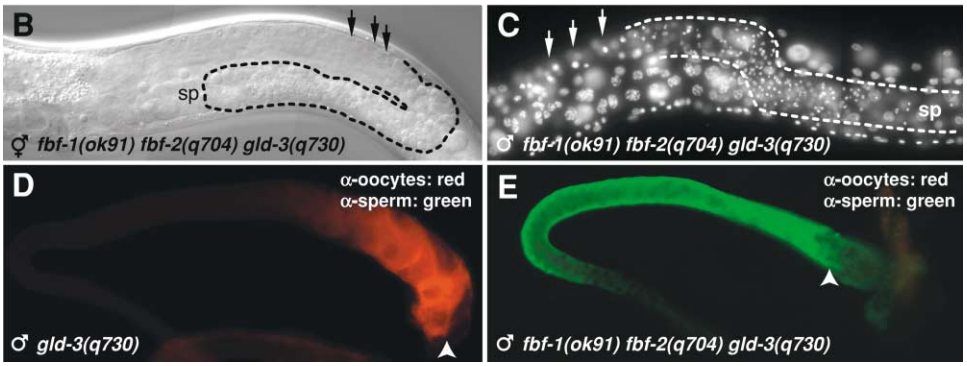

Figure 5. GLD-3 Is a Negative Regulator of FBF

(A) Epistasis analysis of *gld-3* and *fbf*. Top, hermaphrodites; sp, sperm; oo, oocytes. Bottom, males; sp, sperm; oo, oocyte-like cells; n, number of germline arms scored; for *fbf-1 fbf-2* double mutant hermaphrodites, data are from Crittenden et al. (2002). RNAi progeny were scored 12–36 hr postinjection (16°C); triple mutants were scored at 20°C; *gld-3(q730)* homozygotes were derived from *gld-3(q730)/+*.

(B and C) Whole animals; arrows, primary spermatocytes; dashed line, border of region with mature sperm.

(B) *fbf-1(ok91) fbf-2(q704) gld-3(q730)* triple mutant hermaphrodite, Nomarski.

(C) *fbf-1(ok91) fbf-2(q704) gld-3(q730)* triple mutant male, DAPI stained.

(D and E) Extruded germlines stained with both an oocyte-specific antibody (α-RME-2) and a sperm-specific antibody (SP56). Arrowhead marks the proximal end of germline tissue.

(D) *gld-3(q730)* male germline. Oocyte-like cells predominate; four sperm were detected using the SP56 antibody, but they are not visible in this image.

(E) *fbf-1(ok91) fbf-2(q704) gld-3(q730)* triple mutant male. Sperm extend throughout the germline; no oocytes are made. The *fbf-1(ok91) fbf-2(q704)* double mutant has the same staining pattern (not shown).

germline proliferation (Crittenden et al., 2002). However, sufficient germ cells are made in both hermaphrodites and males to assess the sperm/oocyte effect.

In both sexes, we find that *fbf* is epistatic to *gld-3* (Figure 5). Thus, whereas *gld-3* mutant hermaphrodites normally make sperm and oocytes (this work) and *fbf*-depleted animals make only sperm (Zhang et al., 1997), the *fbf-1 fbf-2 gld-3* triple mutant hermaphrodites make only sperm (Figure 5A). These *fbf-1 fbf-2 gld-3* hermaphrodite germlines stain positively for the sperm-specific antibody SP56, and fail to stain with the oocyte-specific antibody α-RME-2, confirming the switch in sexual fate (data not shown). In males, *gld-3* mutants often make oocyte-like cells and never make sperm continuously (Figure 3H), but the *fbf-1 fbf-2 gld-3* males make only sperm (Figure 5C). Furthermore, whereas *gld-3* mutant males stain positively with the oocyte-specific antibody (Figure 5D), the *fbf-1 fbf-2 gld-3* males stain positively with the sperm-specific antibody and fail to stain with the oocyte-specific antibody (Figure 5E). We conclude that *fbf* germline masculinization is epistatic to *gld-3* germline feminization.

We also examined the maturation of spermatocytes in the *fbf-1 fbf-2 gld-3* triple mutant hermaphrodites. In *fbf*-deficient animals, sperm appear to mature normally (Zhang et al., 1997), whereas in *gld-3* mutants, hermaphrodite sperm are blocked as primary spermatocytes (Figures 3 and 4). In both *gld-3; fbf(RNAi)* and *fbf-1 fbf-2 gld-3* triple mutant hermaphrodites, sperm are no longer arrested, but appear to mature normally (Figure 5B). Therefore, a lack of *fbf* suppresses the spermatocyte block typical of *gld-3* mutant hermaphrodites, suggesting

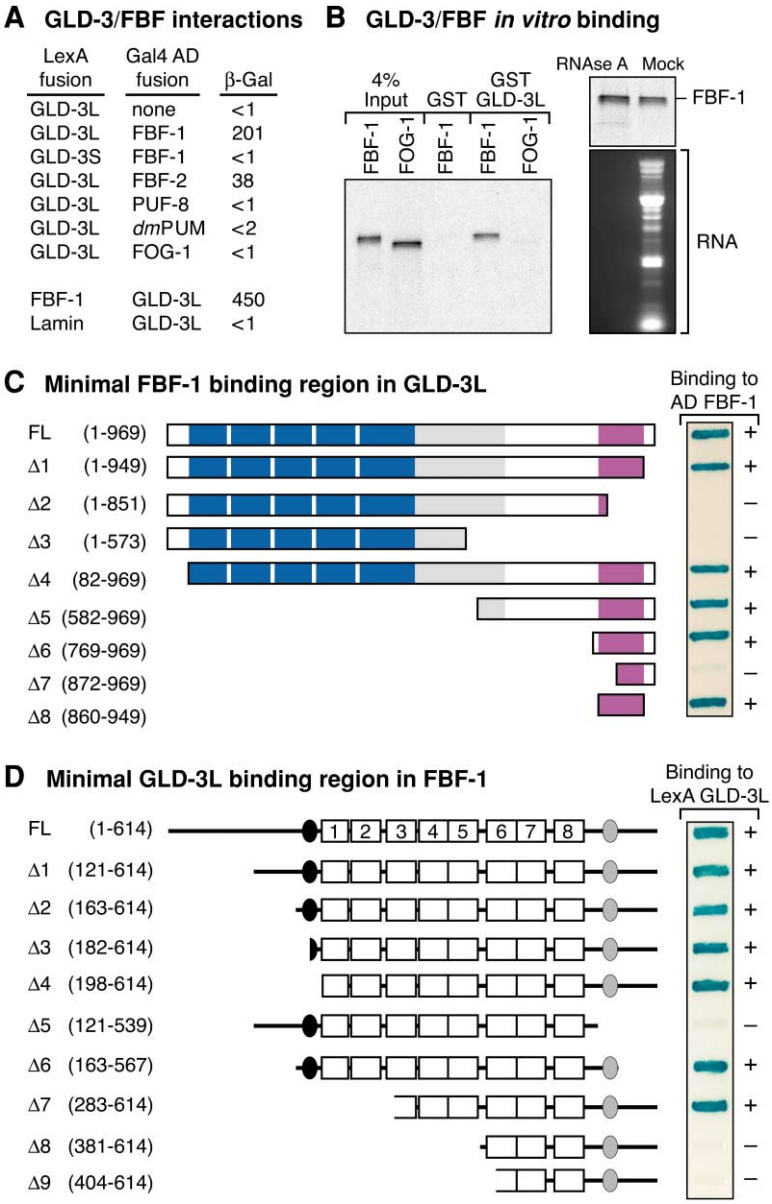

Figure 6. GLD-3 Interacts Specifically with FBF-1

(A) GLD-3L, GLD-3S, FBF-1, FBF-2, PUF-8 (amino acids 143–535), *dm*Pum (amino acids 1091–1426), FOG-1, and Lamin were fused to either the LexA DNA binding domain or the Gal4 transcriptional activation domain (AD) and assayed for interaction using the yeast two-hybrid system. β-galactosidase activity is given in Miller units.

(B) In vitro binding of GLD-3 and FBF. GST/GLD-3L fusion protein and GST alone were immobilized on Sepharose-conjugated glutathione beads and incubated with radiolabeled in vitro-translated FBF-1 or FOG-1. FBF-1 was specifically retained by the GST/GLD-3L fusion protein (left panel). This interaction appears to be RNA independent (right panel). The rabbit reticulocyte lysate was either treated with RNase A or mock incubated without the nuclease before incubation with GST/GLD-3L.

(C) Identification of the region within GLD-3L that binds FBF-1. GLD-3L truncations were fused to the LexA DNA binding domain and tested for their interaction with FBF-1 (amino acids 121–614) fused to the Gal4 transcriptional activation domain (AD). Filter assayed yeast are shown and rated according to their blue color, indicative of β-galactosidase expression levels (+ and − represent strong and weak binding, respectively). GLD-3 motifs follow the codes in Figure 1. A novel 90 amino acid region in the C-terminal region of GLD-3L binds FBF-1.

(D) Identification of the region within FBF-1 that binds to GLD-3L. FBF-1 truncations were fused to the Gal4 activation domain and tested for their interaction with full-length GLD-3L fused to the LexA DNA binding domain. Open boxes, PUF repeats; black and gray ovals, flanking Csp domains. All FBF-1 variants were verified for expression on Western blots.

that a major role of GLD-3 in the maturation of hermaphrodite sperm involves negative regulation of FBF.

GLD-3 and FBF Proteins Interact Specifically

GLD-3 was first identified in a yeast two-hybrid screen as a protein that interacts with FBF-1. To examine the specificity of this interaction, we tested both GLD-3L and GLD-3S for interactions with a variety of PUF proteins (Figure 6A). We found that GLD-3L, but not GLD-3S, was able to bind both FBF-1 and FBF-2. Indeed, the interaction was seen when GLD-3L was fused to the LexA DNA binding domain and FBF-1 to the Gal4 activation domain (AD), or vice versa. Binding of GLD-3L is likely to be similar to FBF-1 and FBF-2: FBF-1 was expressed at about 10-fold higher levels than FBF-2 in two-hybrid tests (Figure 6A and data not shown), perhaps accounting in part for the lower *lacZ* activity with FBF-2 versus FBF-1. Importantly, GLD-3L did not bind either of two other PUF proteins, *C. elegans* PUF-8 or *Drosophila* Pumilio, or to another *C. elegans* RNA binding protein, FOG-1. Therefore, the GLD-3L does not bind PUF proteins nonspecifically, but instead binds to FBF specifically.

We next examined the binding of GLD-3L to FBF-1 in vitro. To this end, we first generated a fusion protein with glutathione S-transferase (GST) fused to GLD-3L. Purified GST/GLD-3L was incubated either with in vitro-translated radiolabeled FBF-1 or another RNA binding protein, FOG-1, and retained proteins were examined by gel electrophoresis (Figure 6B, left panel). We found that GLD-3L retained FBF, but did not retain FOG-1. Therefore, GLD-3L appears to bind FBF specifically in vitro. To test the possibility that the presence of RNA molecules might mediate the observed binding between GLD-3L and FBF-1, we treated the lysate containing ^{35}S-labeled FBF-1 with RNase A before incubation with GST/

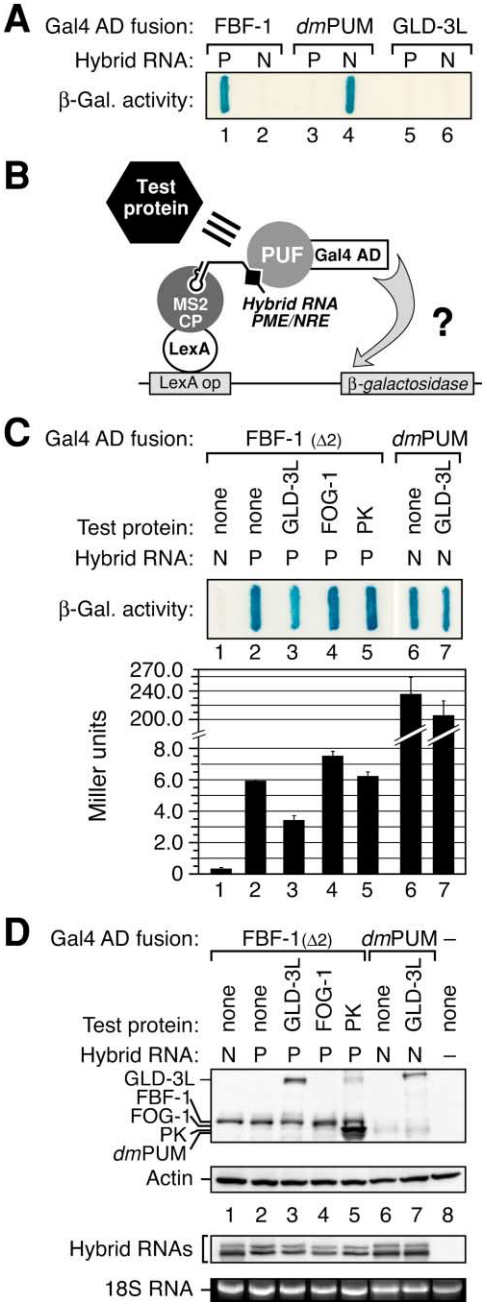

Figure 7. GLD-3 Specifically Reduces FBF Binding to the *fem-3* PME

(A) Yeast three-hybrid assays for binding of FBF-1, *Drosophila* Pumilio (*dm*PUM), and GLD-3 to either of two RNA regulatory elements, the *fem-3* PME (P; Ahringer and Kimble, 1991) or the *hb* NRE (N; Wharton and Struhl, 1991). FBF-1 binds the PME specifically; Pumilio binds the NRE specifically, but GLD-3L binds neither.

(B) Schematic of the modified three-hybrid assay used to test GLD-3L effects on FBF-1 binding. Components include the LexA::MS2 coat protein (CP) fusion, a hybrid RNA (MS2 binding sites fused to either the PME or NRE), and a PUF::Gal4 activation domain fusion. A nonhybrid test protein is added to examine its effect on RNA binding by the PUF protein. Reduced binding is indicated by reduced β-galactosidase activity.

(C) GLD-3L interferes with FBF-1 binding to the PME. Top, filter assayed yeast; bottom, quantitation of β-galactosidase activity. Each filter assay slot is aligned over the bar quantitating that experiment in the graph below; numbers are provided to ensure correct comparisons. Numbered lanes and bars in this panel correspond to numbered lanes in expression controls provided in (D). Gal4 AD fusion proteins: FBF-1 is fragment Δ2 from Figure 6D; *dm*PUM is a fragment of *Drosophila* Pumilio similar to FBF-1Δ2. Test proteins: PK is pyruvate kinase, and FOG-1 is a CPEB-1-related RNA binding protein. Hybrid RNAs: N, NRE; P, PME; lane 1, FBF-1 does not bind the NRE; lane 2, FBF-1 binds the PME; lane 3, GLD-3L reduces FBF-1 RNA binding to the PME by about 2-fold; lanes 4 and 5, neither FOG-1 nor pyruvate kinase (PK) affects the FBF-1/PME interaction; lane 6, *dm*PUM binds the NRE; lane 7, GLD-3L does not affect *dm*PUM/NRE binding.

(D) Expression and loading controls. Lane numbers as in (C). Protein assays: above, Western blot probed for single HA tag fused to each protein. Note that FOG-1 and FBF-1 fusion proteins are almost exactly the same size and appear as one intense band in lane 4. Below, actin provided a loading control. RNA assays: above, Northern blot of total RNA probed for hybrid RNAs. Note that the PME hybrid is slightly larger than the NRE hybrid; doublets are from promiscuous termination by RNA polymerase III. Below, 18S ribosomal RNA provided a loading control.

GLD-3L. Although virtually all RNA has been removed, the physical interaction between GLD-3 and FBF-1 was still observed (Figure 6B, right panel). We conclude that GLD-3 binds specifically to FBF in an RNA-independent fashion.

Finally, we investigated the regions within GLD-3 and FBF-1 critical for their interaction. First, various GLD-3 fragments were tested with FBF-1, defining a domain of 90 amino acids unique to GLD-3L that retained strong FBF-1 binding (Figure 6C). This short FBF binding region bears a novel amino acid sequence that is not found elsewhere in the *C. elegans* genome. Second, various FBF-1 fragments were tested with GLD-3L, defining Puf repeats 3–8 plus the C-terminal Csp domain as essential for the interaction (Figure 6D).

GLD-3 Antagonizes FBF Binding to the *fem-3* 3′UTR Regulatory Element

How might GLD-3 repress FBF activity? One possibility is that GLD-3 might interfere with FBF binding to the PME regulatory element in the *fem-3* 3′UTR. To test this idea, we employed a yeast three-hybrid assay (Sen-Gupta et al., 1996). Briefly, this assay uses three different hybrid molecules to drive transcription of a reporter gene: one hybrid protein carries both a DNA binding domain (e.g., LexA) and an RNA binding domain (e.g., MS2); a second hybrid protein fuses a second RNA binding protein (e.g., FBF-1) to the Gal4 activation domain; and finally, a hybrid RNA (e.g., MS2/PME) bridges the two hybrid RNA binding proteins. We first assayed the binding of FBF-1, *Drosophila* Pumilio, and GLD-3L to either the PME regulatory element of *fem-3* or the NRE of *hb* mRNA. As shown previously (Sonoda and Wharton, 1999; Zhang et al., 1997), FBF-1 bound the PME, but not the NRE (Figure 7A, lanes 1 and 2), and Pumilio bound the NRE, but not the PME (Figure 7A, lanes 3 and 4). Importantly, GLD-3L bound neither the PME nor the NRE (Figure 7A, lanes 5 and 6). Therefore, GLD-3L on its own does not bind specifically to the PME regulatory element of the *fem-3* 3′UTR.

We next used a modified three-hybrid assay to learn whether GLD-3L could interfere with the FBF-1/PME

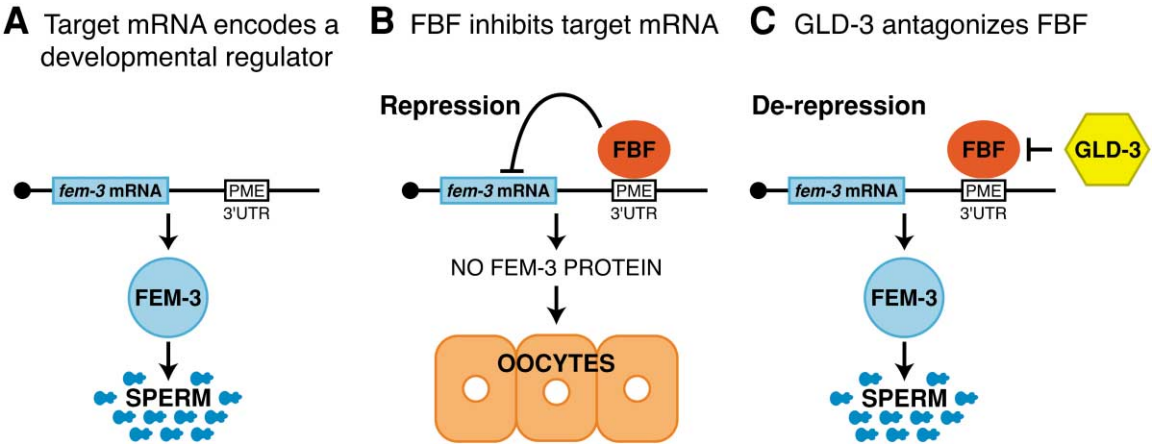

Figure 8. GLD-3 Negatively Regulates FBF to Promote Spermatogenesis

(A) Active *fem-3* mRNA produces FEM-3 protein, which specifies the sperm fate. The PME is a regulatory element located in the *fem-3* 3′UTR.
(B) FBF binds the PME, represses *fem-3* mRNA activity, and blocks production of FEM-3 protein. As a result, spermatogenesis stops and oogenesis begins.
(C) GLD-3 negatively regulates FBF, which derepresses *fem-3* mRNA and promotes spermatogenesis.

interaction. To this end, we introduced into the three-hybrid system a fourth component: a plasmid encoding a test protein (e.g., GLD-3; Figure 7B). We found that FBF-1 bound robustly to the PME as normal in the modified assay (Figure 7C, lane 2), but that binding was attenuated in the presence of GLD-3L (Figure 7C, lane 3). Quantitation showed that introduction of GLD-3L reproducibly reduced β-galactosidase expression by about 2-fold (Figure 7C, bars). Three controls were done to demonstrate that this reduction is specific. First, inhibition required GLD-3L and was not observed when the test protein was an unrelated RNA binding protein (FOG-1; Figure 7C, lane 4) or a different overexpressed protein (PK; Figure 7C, lane 5). Second, GLD-3L did not have a major effect on binding by fly Pumilio to the NRE (Figure 7C, lanes 6 and 7), or binding by yeast Mpt5p/Puf5p to the 3′UTR of HO mRNA (data not shown). Third, the yeast compared in the above experiments were shown to express equivalent levels of the key hybrid proteins (e.g., FBF-1; Figure 7C, lanes 1–5), test proteins (e.g., GLD-3L; Figure 7C, lanes 3 and 7), and hybrid RNAs, and lanes were shown to be loaded equivalently (actin, 18S RNA; Figure 7D). The simplest interpretation of these experiments is that GLD-3L interferes with the FBF-1/PME interaction. Although the effect of GLD-3L on FBF binding is only 2-fold, the reduction is both reproducible and specific. A fourth control experiment to demonstrate specificity was attempted by introducing a truncated version of GLD-3 that lacked its FBF binding region. However, this construct caused a substantial decrease in the amount of hybrid RNA, and therefore was inconclusive. Additional experiments will be required to determine whether GLD-3L affects binding of FBF to the *fem-3* 3′UTR in *C. elegans*.

Discussion

This paper identifies the *C. elegans* GLD-3 protein, characterizes its role in regulating germline development, and explores its functional relationship with two other germline regulators, FBF-1 and FBF-2. GLD-3 belongs to the Bicaudal-C (Bic-C) family of RNA binding proteins. Like Bic-C of *Drosophila* (Saffman et al., 1998 and references therein), GLD-3 has multiple roles in germline development and is also required for embryogenesis. GLD-3 was initially discovered as a two-hybrid interactor with FBF-1, an RNA binding protein of the PUF family. Like GLD-3L, FBF also controls multiple aspects of germline development, including sex determination (Zhang et al., 1997), spermatogenesis (Luitjens et al., 2000), and maintenance of germline stem cells (Crittenden et al., 2002). We have focused on germline sex determination to explore the functional relationship between FBF and GLD-3.

GLD-3 Antagonizes FBF to Control Germline Sex Determination

Normally in *C. elegans*, the hermaphrodite germline makes sperm and then oocytes, whereas males make sperm continuously. In hermaphrodites, the number of sperm made before the transition to oogenesis is roughly the same from individual to individual. The *gld-3* gene promotes the sperm fate: in males, *gld-3* governs the continued production of sperm, and in hermaphrodites, *gld-3* is critical for making the normal number of sperm. We suggest here that *gld-3* exerts its control over germline sex determination by modulating FBF activity.

The FBF RNA binding proteins normally promote oogenesis by inhibiting *fem-3* mRNA, which encodes a sperm-promoting activity (Zhang et al., 1997). In the absence of FBF, *fem-3* mRNA makes FEM-3 protein, which directs the sperm fate (Figure 8A); in the presence of FBF, *fem-3* mRNA is repressed and oogenesis ensues (Figure 8B). GLD-3 promotes the sperm fate, an effect opposite to that of FBF. Double mutant experiments show that FBF is epistatic to GLD-3: when FBF is removed, GLD-3 is no longer required for specification of the sperm fate. Therefore, GLD-3 is likely to act upstream of FBF to inhibit or antagonize FBF activity (Figure 8C).

The FBF regulation by GLD-3 plays a key role in controlling germline sexual fates. FBF normally remains active in the mature germline to promote stem cells (Crittenden et al., 2002) and therefore must be inhibited to make sperm. We suggest that GLD-3 is a major inhibitor of FBF, and that GLD-3 normally inhibits FBF to permit spermatogenesis in both sexes. However, other FBF inhibitors are likely to exist, because most hermaphrodites and males make some sperm before switching to oogenesis in the absence of GLD-3.

FBF and GLD-3 Control Overlapping, But Not Identical, Aspects of Development

The biological processes regulated by GLD-3 and FBF are overlapping, but not identical. Maternally, GLD-3 is required for both embryogenesis and germline survival; zygotically, GLD-3 is required for germline sex determination (see above) and for the processes of both oogenesis and spermatogenesis. By contrast, FBF has no known role in embryogenesis or oogenesis; instead, FBF controls germline stem cell maintenance (Crittenden et al., 2002) and germline sex determination (see above), and appears to be critical for the process of spermatogenesis (Luitjens et al., 2000).

The maternal GLD-3 functions in early embryogenesis, and germline survival cannot be easily explained by a relationship with FBF. FBF has no known effect in early embryogenesis, and FBF protein is not detectable in oocytes or early embryos. Furthermore, although FBF has been implicated in germline survival (Subramaniam and Seydoux, 1999), its germline survival defects were observed in animals depleted for FBF plus four other PUF proteins. One possible explanation for the *gld-3* germline survival defect may be that maternal GLD-3 acts in the P4 blastomere or its descendants for early germline functions. Consistent with this idea, GLD-3 colocalizes with P granules, which have been implicated in germline specification (Seydoux and Strome, 1999). Although no other PUF protein has been identified to date as a GLD-3 interactor (C.R.E., unpublished data), we cannot exclude the possibility that GLD-3 may antagonize other PUF proteins for these maternal functions. Alternatively, GLD-3 may act independently of PUF proteins in the early embryo. A parallel study has revealed that GLD-3 binds to another germline regulator, GLD-2, which colocalizes with P granules and is required maternally for early embryogenesis (Wang et al., 2002). Therefore, GLD-3 may act with GLD-2 rather than with FBF in the early embryo.

How Does GLD-3 Inhibit FBF at the Molecular Level?

The molecular mechanism by which GLD-3 opposes FBF is not understood, but several findings provide clues. First, GLD-3 and FBF are both cytoplasmic proteins that are expressed in the germline (this work; Zhang et al., 1997). Although FBF is expressed in the germline mitotic region (Crittenden et al., 2002) and GLD-3 is expressed in the transition zone and oocytes (Figure 2), their expression overlaps in the proximal mitotic region and transition zone, indicating that GLD-3 may interact directly with FBF in *C. elegans*. The narrow region of overlap suggests that only a minority of FBF and GLD-3 protein molecules interact. Second, GLD-3 binds specifically to FBF. For example, GLD-3 binds both FBF-1 and FBF-2, but not other PUF proteins (Figure 6). Third, GLD-3 appears to interfere with FBF binding to the *fem-3* PME 3′UTR regulatory element (Figure 7). Putting these findings together, we suggest that GLD-3 antagonizes FBF by a mechanism relying on direct interaction between the two proteins. The GLD-3/FBF interaction may release target mRNAs from FBF repression, or it may alter FBF binding to RNA or other interactors (e.g., NOS-3; Kraemer et al., 1999). A more radical possibility is that GLD-3 may be recruited to target mRNAs by FBF and then actively promote translation, reversing the effect of FBF. Recent studies have shown that GLD-3 binds and stimulates the activity of another germline regulatory protein called GLD-2, a regulatory cytoplasmic poly(A) polymerase (Wang et al., 2002). Therefore, GLD-3 may antagonize FBF by promoting polyadenylation of its target mRNAs. Challenges for the future include determining the mechanism of antagonism and learning the extent to which the regulatory relationship between PUF and Bic-C family members has been conserved.

Experimental Procedures

Strains

The following mutations were used: *LGI*: *smg-1(r681)*, *LGII*: *fbf-1(ok91)*, *fbf-2(q704)*, *gld-3(q730)*; *LGIII*: *unc-32(e189)*, *glp-1(q224)*; *LGIV*: *ced-3(n717)*; *LGV*: *rde-1(ne219)*. Rearrangements: *mnIn1[mIs14 dpy-10(e128)]* (*LGII*).

Sequence Analysis of *gld-3* and *bcc-1*

gld-3L, *gld-3S*, and *bcc-1* correspond to the predicted genes T07F8.3a, T07F8.3b, and M7.3, respectively. The intron/exon boundaries and the SL1 *trans*-spliced leader were determined by sequencing cDNAs of *gld-3* (yk351f11, yk345b5, GLP5[pJK846]) and various RT-PCR-generated clones for *gld-3* and *bcc-1*. RT-PCR experiments and phylogenetic analysis are explained in Supplemental Procedures.

RNA Interference

For RNAi of *gld-3*, we injected a double-stranded (ds) RNA corresponding to nucleotides (nt) 1–2847 into wild-type adult hermaphrodite germlines at a concentration of 0.5 mg/ml. For zygotic RNAi, we injected *unc-32; rde-1* hermaphrodites and crossed them with wild-type males to score crossprogeny. Double RNAi experiments were done by coinjecting a mixture of dsRNAs corresponding to *fbf-1* (nt 363–1842) and *gld-3* (nt 1–1719) at a final concentration of 0.5 mg/ml each. Detailed information is in Supplemental Procedures.

Two-Hybrid Screen/Assays and GST-FBF Protein Affinity Chromatography

The initial yeast two-hybrid screen with FBF-1 has been described previously (Kraemer et al., 1999). Derivatives of *gld-3L* in pBTM116 and FBF-1 in pACTII were made by utilizing convenient restriction sites. Affinity chromatography experiments were performed essentially as described (Kraemer et al., 1999). ^{35}S-radiolabeled FBF-1 and FOG-1 were prepared by priming the T7 TNT-coupled reticulocyte lysate transcription/translation system (Promega) separately with cDNAs inserted into the pCITE-4 vector system (Novagen).

Three-Hybrid Assays

Three-hybrid experiments and assays were performed as described (Bernstein et al., 2002). The RNA sequences for PME in pIIIA/MS2-2 and NRE in pIII/MS2-2 and HO 3′UTR/MS2-2 were described previously (Sonoda and Wharton, 1999; Tadauchi et al., 2001; Zhang et al., 1997). These RNAs were cotransformed with either FBF-1 (amino acids 163–614), *dm*PUM (amino acids 1091–1426), or GLD-3L (amino acids 1–949) in pACT/pACTII vectors into YBZ-1.

Hybrid protein and hybrid RNA constructs to test proteins interfering with the observed RNA/protein interactions are explained in Supplemental Procedures. All constructs expressing GLD-3L, FOG-1, or PK were cotransformed together with FBF-1 or *dm*PUM and the hybrid RNAsΔUra (PME or NRE) into YBZ-1. Total protein and RNA extracts from logarithmically grown yeast cells were prepared according to standard techniques. For Northern analysis, we used an RNA antisense probe against the MS-2 binding sites (pTET-2 MS2; SenGupta et al., 1996). For Western analysis, we used the anti-HA 12CA5 (1:2,000 dilution) and the anti-Actin antibody C4 (1:25,000 dilution). Levels of β-galactosidase were assayed in at least two independent experiments from four to eight independent transformants.

GLD-3 Antibodies

Polyclonal antibodies were made against the N-terminal peptide (amino acids 2–24; anti-GLD-3) and the C-terminal fragment of GLD-3L (amino acids 582–949; anti-GLD-3L) fused to GST. Further information is available in Supplemental Procedures.

Acknowledgments

We thank Yuji Kohara for cDNA clones, Mike Krause for the partial actin-1 cDNA, Elizabeth Craig for yeast expression plasmids, Gideon Dreyfuss for chicken muscle pyruvate kinase (PK) cDNA, Barth Grant for anti-RME-2, Susan Strome for anti-PGL-1, Sam Ward for the sperm-specific antibody SP56, and Craig Mello, Phil Anderson, and the *Caenorhabditis* Genetics Center (CGC) for providing strains. We thank members of the Kimble and Wickens laboratories for comments on the manuscript. We are also grateful to Peggy Kroll-Conner for assistance with generating the *gld-3* deletion mutant, and Anne Helsley-Marchbanks and Laura Vanderploeg for help with preparing the manuscript and figures. C.R.E. was supported by a long-term fellowship of the Human Frontier Science Program (HFSP). M.W. is supported by the National Institutes of Health (NIH). J.K. is an investigator with the Howard Hughes Medical Institute (HHMI).

Received: April 17, 2002
Revised: September 6, 2002

References

Ahringer, J., and Kimble, J. (1991). Control of the sperm-oocyte switch in *Caenorhabditis elegans* hermaphrodites by the *fem-3* 3′ untranslated region. Nature *349*, 346–348.

Barton, M.K., and Kimble, J. (1990). *fog-1*, a regulatory gene required for specification of spermatogenesis in the germ line of *Caenorhabditis elegans*. Genetics *125*, 29–39.

Bernstein, D.S., Buter, N., Stumpf, C., and Wickens, M. (2002). Analyzing mRNA-protein complexes using a yeast three-hybrid system: methods and applications. Methods *26*, 123–141.

Crittenden, S.L., Bernstein, D.S., Bachorik, J.L., Thompson, B.E., Gallegos, M., Petcherski, A.G., Moulder, G., Barstead, R., Wickens, M., and Kimble, J. (2002). A conserved RNA-binding protein controls germline stem cells in *Caenorhabditis elegans*. Nature *417*, 660–663.

Dever, T.E. (2002). Gene-specific regulation by general translation factors. Cell *108*, 545–556.

Ellis, H.M., and Horvitz, H.R. (1986). Genetic control of programmed cell death in the nematode *C. elegans*. Cell *44*, 817–829.

Francis, R., Barton, M.K., Kimble, J., and Schedl, T. (1995). *gld-1*, a tumor suppressor gene required for oocyte development in *Caenorhabditis elegans*. Genetics *139*, 579–606.

Goodwin, E.B., Okkema, P.G., Evans, T.C., and Kimble, J. (1993). Translational regulation of *tra-2* by its 3′ untranslated region controls sexual identity in *C. elegans*. Cell *75*, 329–339.

Grant, B., and Hirsh, D. (1999). Receptor-mediated endocytosis in the *Caenorhabditis elegans* oocyte. Mol. Biol. Cell *10*, 4311–4326.

Hengartner, M.O. (1997). Cell death. In *C. elegans* II, J.R. Priess, ed. (Cold Spring Harbor, NY: Cold Spring Harbor Laboratory Press), pp. 383–415.

Jin, S.-W., Kimble, J., and Ellis, R.E. (2001). Regulation of cell fate in *Caenorhabditis elegans* by a novel cytoplasmic polyadenylation element binding protein. Dev. Biol. *229*, 537–553.

Kadyk, L.C., and Kimble, J. (1998). Genetic regulation of entry into meiosis in *Caenorhabditis elegans*. Development *125*, 1803–1813.

Kawasaki, I., Shim, Y.-H., Kirchner, J., Kaminker, J., Wood, W.B., and Strome, S. (1998). PGL-1, a predicted RNA-binding component of germ granules, is essential for fertility in *C. elegans*. Cell *94*, 635–645.

Kimble, J.E., and White, J.G. (1981). On the control of germ cell development in *Caenorhabditis elegans*. Dev. Biol. *81*, 208–219.

Kraemer, B., Crittenden, S., Gallegos, M., Moulder, G., Barstead, R., Kimble, J., and Wickens, M. (1999). NANOS-3 and FBF proteins physically interact to control the sperm-oocyte switch in *Caenorhabditis elegans*. Curr. Biol. *9*, 1009–1018.

Labouesse, M., Sookhareea, S., and Horvitz, H.R. (1994). The *Caenorhabditis elegans* gene *lin-26* is required to specify the fates of hypodermal cells and encodes a presumptive zinc-finger transcription factor. Development *120*, 2359–2368.

Luitjens, C., Gallegos, M., Kraemer, B., Kimble, J., and Wickens, M. (2000). CPEB proteins control two key steps in spermatogenesis in *C. elegans*. Genes Dev. *14*, 2596–2609.

Mahone, M., Saffman, E.E., and Lasko, P.F. (1995). Localized *Bicaudal-C* RNA encodes a protein containing a KH domain, the RNA binding motif of FMR1. EMBO J. *14*, 2043–2055.

Meyer, B.J. (1997). Sex determination and X chromosome dosage compensation. In *C. elegans* II, J.R. Priess, ed. (Cold Spring Harbor, NY: Cold Spring Harbor Laboratory Press), pp. 209–240.

Murata, Y., and Wharton, R. (1995). Binding of Pumilio to maternal *hunchback* mRNA is required for posterior patterning in *Drosophila* embryos. Cell *80*, 747–756.

Nakahata, S., Katsu, Y., Mita, K., Inoue, K., Nagahama, Y., and Yamashita, M. (2001). Biochemical identification of *Xenopus* Pumilio as a sequence-specific cyclin B1 mRNA-binding protein that physically interacts with a Nanos homolog, Xcat-2, and a cytoplasmic polyadenylation element-binding protein. J. Biol. Chem. *276*, 20945–20953.

Pulak, R., and Anderson, P. (1993). mRNA surveillance by the *Caenorhabditis elegans smg* genes. Genes Dev. *7*, 1885–1897.

Puoti, A., Gallegos, M., Zhang, B., Wickens, M.P., and Kimble, J. (1997). Controls of cell fate and pattern by 3′ untranslated regions: the *Caenorhabditis elegans* sperm/oocyte decision. Cold Spring Harb. Symp. Quant. Biol. *62*, 19–24.

Saffman, E.E., Styhler, S., Rother, K., Li, W., Richard, S., and Lasko, P. (1998). Premature translation of *oskar* in oocytes lacking the RNA-binding protein Bicaudal-C. Mol. Cell. Biol. *18*, 4855–4862.

SenGupta, D.J., Zhang, B., Kraemer, B., Pochart, P., Fields, S., and Wickens, M. (1996). A three-hybrid system to detect RNA-protein interactions in vivo. Proc. Natl. Acad. Sci. USA *93*, 8496–8501.

Seydoux, G., and Strome, S. (1999). Launching the germline in *Caenorhabditis elegans*: regulation of gene expression in early germ cells. Development *126*, 3275–3283.

Sonoda, J., and Wharton, R.P. (1999). Recruitment of Nanos to *hunchback* mRNA by Pumilio. Genes Dev. *13*, 2704–2712.

Subramaniam, K., and Seydoux, G. (1999). *nos-1* and *nos-2*, two genes related to *Drosophila nanos*, regulate primordial germ cell development and survival in *Caenorhabditis elegans*. Development *126*, 4861–4871.

Tabara, H., Sarkissian, M., Kelly, W.G., Fleenor, J., Grishok, A., Timmons, L., Fire, A., and Mello, C.C. (1999). The *rde-1* gene, RNA interference, and transposon silencing in *C. elegans*. Cell *99*, 123–132.

Tadauchi, T., Matsumoto, K., Herskowitz, I., and Irie, K. (2001). Post-transcriptional regulation through the HO 3′-UTR by Mpt5, a yeast homolog of Pumilio and FBF. EMBO J. *20*, 552–561.

Wang, L., Eckmann, C.R., Kadyk, L.C., Wickens, M., and Kimble, J. (2002). A regulatory cytoplasmic poly(A) polymerase in *C. elegans*. Nature *419*, 312–316.

Ward, S., Roberts, T.M., Strome, S., Pavalko, F.M., and Hogan, E.

(1986). Monoclonal antibodies that recognize a polypeptide antigenic determinant shared by multiple *Caenorhabditis elegans* sperm-specific proteins. J. Cell Biol. *102*, 1778–1786.

Wessely, O., and De Robertis, E.M. (2000). The *Xenopus* homologue of *Bicaudal-C* is a localized maternal mRNA that can induce endoderm formation. Development *127*, 2053–2062.

Wessely, O., Tran, U., Zakin, L., and De Robertis, E.M. (2001). Identification and expression of the mammalian homologue of *Bicaudal-C*. Mech. Dev. *101*, 267–270.

Wharton, R.P., and Struhl, G. (1991). RNA regulatory elements mediate control of *Drosophila* body pattern by the posterior morphogen *nanos*. Cell *67*, 955–967.

Wharton, R.P., Sonoda, J., Lee, T., Patterson, M., and Murata, Y. (1998). The Pumilio RNA-binding domain is also a translational regulator. Mol. Cell *1*, 863–872.

Wickens, M., Goodwin, E.B., Kimble, J., Strickland, S., and Hentze, M.W. (2000). Translational control in developmental decisions. In Translational Control of Gene Expression, N. Sonenberg, ed. (Cold Spring Harbor, NY: Cold Spring Harbor Laboratory Press), pp. 295–370.

Wickens, M., Bernstein, D.S., Kimble, J., and Parker, R. (2002). A PUF family portrait: 3′UTR regulation as a way of life. Trends Genet. *18*, 150–157.

Zalevsky, J., MacQueen, A.J., Duffy, J.B., Kemphues, K.J., and Villeneuve, A.M. (1999). Crossing over during *Caenorhabditis elegans* meiosis requires a conserved MutS-based pathway that is partially dispensable in budding yeast. Genetics *153*, 1271–1283.

Zamore, P.D., Williamson, J.R., and Lehmann, R. (1997). The Pumilio protein binds RNA through a conserved domain that defines a new class of RNA-binding proteins. RNA *3*, 1421–1433.

Zhang, B., Gallegos, M., Puoti, A., Durkin, E., Fields, S., Kimble, J., and Wickens, M.P. (1997). A conserved RNA-binding protein that regulates sexual fates in the *C. elegans* hermaphrodite germ line. Nature *390*, 477–484.